Structural and magnetic properties of ultrathin fcc Fe_xMn_{1-x} films on Cu(100)

R. Thamankar, S. Bhagwat, and F. O. Schumann
Freie Universität Berlin, Institut für Experimentalphysik, Arnimallee 14, 14195 Berlin, Germany
(Received 24 September 2003; published 17 February 2004)

We have studied ultrathin Fe_xMn_{1-x} films on Cu(100) for Fe contents ranging from 45% to 80%. In the bulk the fcc structure displays antiferromagnetic order in this concentration regime. The growth was investigated via reflection high energy electron diffraction and structural properties were investigated with low energy electron diffraction. From lattice mismatch arguments one would have expected to observe a $p(1\times1)$ pattern. However we find a $c(2\times2)$ structure for thicknesses below 5 ML. Above this coverage it transforms into a $p(1\times1)$ structure. The $c(2\times2)$ structure is not present when the alloys are grown on a Co/Cu(100) surface. With the use of Auger spectroscopy we find clear evidence of Fe surface segregation. At 54% Fe content we estimate an enhancement of the surface content of Fe by $\sim10\%$. The amount of excess Fe agrees well with the observation of 'uncompensated' Fe spins in $Co/Fe_{50}Mn_{50}$ structures. Further we were able to detect magnetic signals for coverages below ~5 ML.

DOI: 10.1103/PhysRevB.69.054411 PACS number(s): 75.70.Ak, 75.50.Bb, 75.70.Rf

I. INTRODUCTION

In exchange-bias systems the antiferromagnetic layer material often consists of a $Fe_{50}Mn_{50}$ alloy since at this content the Néel temperature T_N is largest. The exchange bias is due to the exchange interaction at the interface ferromagnet-antiferromagnet.[1] Discussions of the exchange bias often assume the magnetic structure of the bulk due to the lack of experimental results about the surface/interface. However it has been recently demonstrated that the situation at the surface is different from the bulk in the system Co/NiO(100).[2] The materials used for the antiferromagnetic layer in exchange-bias systems can be roughly divided into two groups.[1] One class consists of oxides, and examples are CoO and NiO. The other class contains Mn alloys, like FeMn and IrMn. The important fact is that the antiferromagnetic layer material is not a single element, but some chemical compound. Growing the ferromagnet onto the oxide will cause oxidation-reduction reactions modifying the interface responsible for the exchange interaction.[3,4] On the other hand, when growing alloy films one has to address the question of surface segregation as observed, for example, in Fe_xNi_{1-x} in bulk and thin film samples.[5–7] This means the interface which is important for the exchange interaction cannot simply be derived from a bulk terminated surface. It is also well known that due to the lattice misfit between film and substrate a tetragonally distorted structure evolves, e.g., Co and Ni/Cu(100) films.[8,9] This change of symmetry could have an impact on the exchange interaction. It is therefore imperative to address the chemical and structural properties of antiferromagnetic ultrathin films. Surprisingly very few studies have been performed addressing these issues. In the following we want to discuss Fe_xMn_{1-x} alloys grown on Cu(100). On the basis of bulk lattice constants of fcc Fe_xMn_{1-x} alloys[10] we have calculated the misfit when grown on a Cu(100) surface; see Fig. 1. The value ranges from -0.8% to 0.5%, and therefore a Cu(100) surface is a good choice as a substrate and we expect pseudomorphic growth. In the bulk Fe_xMn_{1-x} alloys display complex structural and magnetic behaviors, which we briefly review via a simplified phase diagram in Fig. 1.

The fcc phase is stable for Fe contents between 80% and 50%. There the Néel temperature T_N increases monotonically as a function of the Mn content. A sample with 20% Mn has a value of T_N of ~360 K compared to ~500 K for 50% Mn. For Fe contents above 90% Fe_xMn_{1-x} is in a bcc phase, which displays a ferromagnetic behavior. The Curie temperature T_C decreases linearly in this regime and at 90%

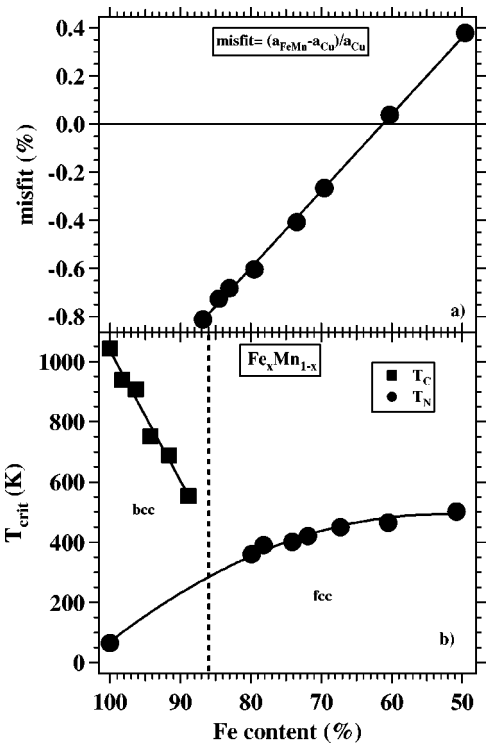

FIG. 1. The top panel displays the misfit of fcc Fe_xMn_{1-x} on Cu(100) using bulk lattice constants (Ref. 10). The bottom panel shows a simplified phase diagram and critical temperatures for bulk Fe_xMn_{1-x} (Refs. 11 and 13). The dashed lines separate fcc and bcc phases. The solid lines serve as a guide for the eye.

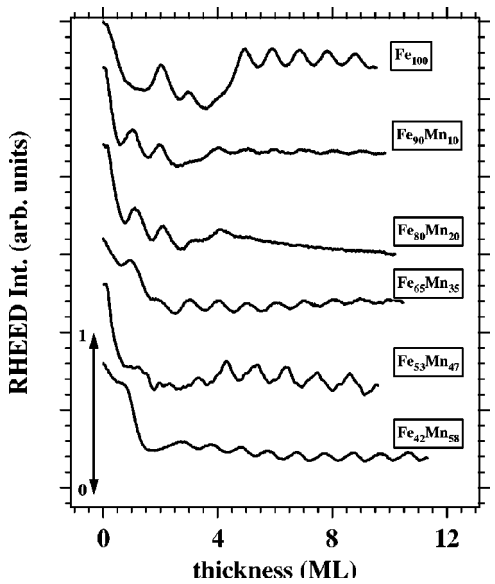

FIG. 2. RHEED Intensity variations during growth for different Fe_xMn_{1-x} alloy films.

Fe T_C is around 500 K, which is ~50% of the value of bcc Fe.[11] The T_N value for fcc Fe stems from measurements of fcc Fe precipitates in a Cu matrix.[12] We want to address the following questions. (i) How does the growth of Fe_xMn_{1-x} films proceed on a Cu(100) surface? (ii) What is the structure of these films? (iii) Does surface segregation play a role? (iv) Can magnetic order be directly observed?

II. EXPERIMENT

The experiments were performed in an ultra high vacuum chamber (1×10^{-10} mbar) equipped with a LEED (low electron energy diffraction) optics for structural analysis and CMA (cylindrical mirror analyzer) for chemical analysis. A second electron gun for reflection high energy electron diffraction (RHEED) studies during the growth is available. E-beam sources were used for the deposition of Fe and Mn. The rate of all evaporators can be controlled by individual quartz crystal monitors. In order to calibrate these thickness monitors we used RHEED oscillations, which are well documented for Fe/Cu(100).[14,15] The calibration of the Mn evaporator is not so straight-forward since no RHEED oscillations for Mn/Cu(100) exist. We adopted the following procedure for calibration of the Mn source. Similar to the recent observations of Offi et al. we observed RHEED oscillations for a ~$Fe_{50}Mn_{50}$ alloy during the growth on Cu(100); see Fig. 2.[16] From this experiment we can determine the total thickness of the alloy film. Since the Fe source is already calibrated we know the amount of Fe deposited. From the difference of the total thickness and the Fe contribution we can calculate the Mn contribution. This gives us the calibration value for the Mn source. Additionally we use Auger spectroscopy to determine the Fe concentration. Since we know the Fe amount we can determine the Mn contribution to yield the concentration measured with Auger spectroscopy, independently confirming the result from the RHEED experiment. In regular intervals the calibration values were checked, which we found to be stable within 5%. A well ordered Cu(100) surface was prepared via Ar^+ sputtering and annealing to 720 K. Alloy films were deposited at 300 K by simultaneous deposition at a rate of ~0.2 ML/min. At present the lowest temperature we can achieve is 110 K with LN_2 cooling. For magnetic measurements we utilized the magneto-optical Kerr effect (MOKE), our setup allows to perform these experiments at the growth position. The in-plane and out-of-plane magnetization can be probed by orthogonal magnets. Therefore no sample movement is necessary for Kerr measurements along two directions. The maximum available field is at present ~1000 G. We prepared uniform and wedged samples, both sets gave identical results. For the wedges we placed the Cu(100) crystal behind a shutter. During the growth we varied the *z* position of the sample via a stepper motor. The slope was typically ~1 ML/mm. The size of the light spot is ~0.25 mm, which gives us a thickness resolution of ~0.25 ML. The positioning error in the MOKE position is at most ~0.5 mm, which results in a thickness error of ~0.5 ML.

III. GROWTH OF FCC Fe_XMn_{1-x}/Cu(100) FILMS

From the lattice mismatch argument [see Fig. 1(a)] we expect good epitaxial growth of Fe_xMn_{1-x} on Cu(100). In order to study the growth we recorded the RHEED intensity during evaporation. The results for different concentrations are plotted in Fig. 2. All curves are normalized such that at the beginning of the growth the RHEED intensity is 1. Further we plotted all curves in the intensity interval 0.2–1. Only then one can compare these curves. The behavior of Fe/Cu(100) is well studied and our intensity curve is in agreement with published data. The main features are a missing peak at the 1-ML position and a significant increase of the intensity at ~4 ML, where RHEED oscillations also set in. This we could use for the calibration of the Fe source. For 90% Fe we observe a maximum at the 1-ML position and oscillations are pronounced for the first 2 ML. At 3 ML only a weak peak is present, and finally at ~4 ML we notice an increase in the intensity. RHEED oscillations are present beyond this thickness. However the amplitude is smaller when compared with Fe/Cu(100). The intensity curve for a Fe_{80} alloy is similar except that beyond 4 ML no oscillations are detectable. At 65% Fe we notice a rapid decrease of the intensity once the growth has commenced. Oscillations in the RHEED intensity are detectable up to ~10 ML. For an Fe content of 53% the RHEED intensity drops rapidly but for thicknesses above 4 ML RHEED oscillations are found. The amplitude of the oscillations is of the same order as for Fe/Cu(100). Our observations regarding the growth of Fe_xMn_{1-x} on Cu(100) are in line with the findings of Offi and co-workers.[16,17] We conclude that Fe_xMn_{1-x} alloys on Cu(100) are a good epitaxial system.

IV. STRUCTURAL ASPECTS OF Fe_XMn_{1-x}/Cu(100) FILMS

Due to the small lattice mismatch between Fe_xMn_{1-x} alloys and Cu(100) we expect pseudomorphic growth; see Fig.

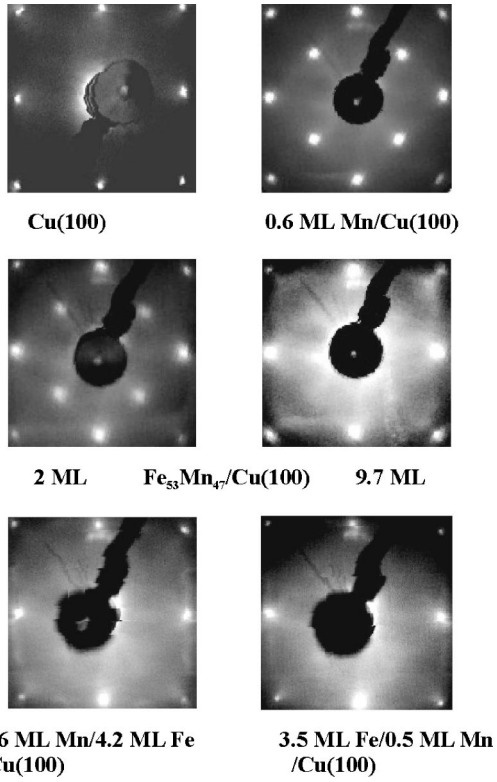

FIG. 3. Various LEED patterns obtained at 110 eV.

1(a). Hence we expect LEED images of $p(1\times1)$ symmetry like the substrate. In particular we should not observe reconstructions. In Fig. 3 we display LEED images obtained at an electron energy of $\sim$110 eV. The Cu(100) surface displays the known $p(1\times1)$ symmetry. This we can compare with the pattern of 2 ML $Fe_{53}Mn_{47}$. We immediately notice extraspots, which are of $c(2\times2)$ symmetry. Increasing the thickness to 9.7 ML leads to a $p(1\times1)$ pattern, as expected. The transition from a $c(2\times2)$ pattern to a $p(1\times1)$ pattern takes place between 4 and 6.4 ML for an $Fe_{53}Mn_{47}$ alloy. This type of behavior has been observed for all concentrations in the regime 50–75 % Fe. A similar transition from a $c(2\times2)$ to $p(1\times1)$ structure was reported in related systems like Mn/Cu(100) and Mn/Pd(100).[18–21]

The question arises what is the origin of the $c(2\times2)$ structure. We recall results of so-called surface alloys which are present for 0.5 ML Mn/Cu(100) and 0.5 ML Mn/Ni/Cu(100). There the toplayer consists of an ordered alloy with a $c(2\times2)$ LEED pattern, which we are able to reproduce; see Fig. 3.[20,22] In this structure a significant buckling of the Mn atoms occurs.[20] More precisely the Mn atoms have a different displacement along the surface normal than the Cu atoms.[20] Therefore two possibilities for the observed $c(2\times2)$ structure in $Fe_{53}Mn_{47}$ are conceivable: (1) significant surface segregation of Mn, which forms a surface alloy like Mn/Cu(100); and (2) the formation of a Mn/Cu(100) alloy at the interface. We have grown 0.5 ML Mn on 4.2 ML Fe/Cu(100), and observed a $p(1\times1)$ pattern with some faint intensity due to a 5×1 reconstruction similar to Fe/Cu(100); see Fig. 3.[14,23] Therefore we dismiss the first possibility. Next we investigated 3.5 ML Fe on a $c(2\times2)$ Mn/Cu(100) surface. At this coverage the $c(2\times2)$ structure is buried; see Fig. 3. This in contrast to 4-ML $Fe_{53}Mn_{47}$, where a $c(2\times2)$ pattern is clearly visible. Therefore the formation of a MnCu alloy is not likely. In a next step we collected *I-V* data on the $(\frac{1}{2}\frac{1}{2})$ spots, which are plotted in Fig. 4. The top curve is from 0.5 ML Mn/Cu(100) in agreement with Wuttig *et al.*[20] Growth of Fe on this sample leaves the shape of the *I-V* curve almost unaffected. The important observation is that the curve of 2 ML $Fe_{50}Mn_{50}$ is also very similar to the curve of 0.5 ML Mn/Cu(100). This is strong evidence that a buckling of Mn is important for the $c(2\times2)$ structure in our alloy films. Having said that an ordered alloy could account for the presence of a $c(2\times2)$ structure, it becomes clear this is at odds with an uniform sample. A ''perfect'' $c(2\times2)$ structure is equivalent to an Fe content of 50%. However, samples with a higher Fe content also displayed the $c(2\times2)$ pattern. This suggests that some Fe has to segregate to the surface or Cu interface. We will show below that indeed Fe surface segregation occurs. In Fig. 5 we have summarized our findings with respect to superstructures in the LEED pattern. For completeness sake we have included experimental results on Fe-rich Fe_xMn_{1-x} alloys.[24] In the interval 100–75 % Fe we observed up to $\sim$5 ML a $n\times1$ pattern, with $n\sim5$.[23] Exceeding a thickness of $\sim$5 ML results in a 2×1 pattern. A solid line marks the boundary of these two regimes. At about 75% Fe the symmetry of the LEED pattern changes significantly, and we placed a vertical dashed line in the diagram. For Fe contents below 75% we observe a $c(2\times2)$ pattern as discussed above for the special case of $Fe_{53}Mn_{47}$. At 10 ML this pattern has transformed into a $p(1\times1)$ pattern. A second solid line separates these two regimes. Our findings on Fe_xMn_{1-x}/Cu(100) do not agree in every aspect with the recent reports by Offi *et al.*[16] They focus in their work on $Fe_{50}Mn_{50}$ alloys and report only a $p(1\times1)$ structure. The preparation is different only in two aspects. First, we grow our samples at 300 K whereas, Offi

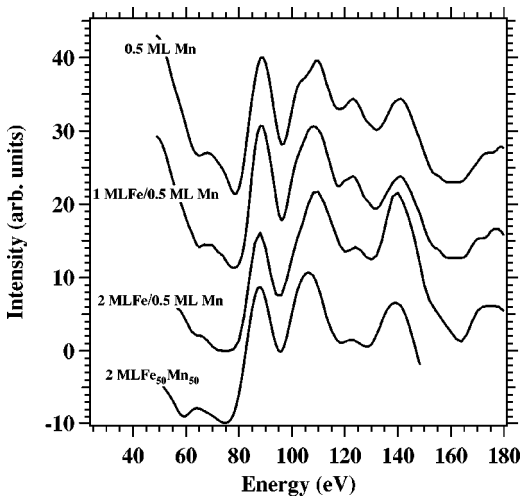

FIG. 4. LEED *I-V* curves of the $(\frac{1}{2}\frac{1}{2})$ spots. We compare 0.5-ML Mn/Cu(100) at various stages during the Fe overlayer growth with 2 ML $Fe_{50}Mn_{50}$. The intensities have been scaled such the spectra are of equal height. We note a close resemblance of these curves.

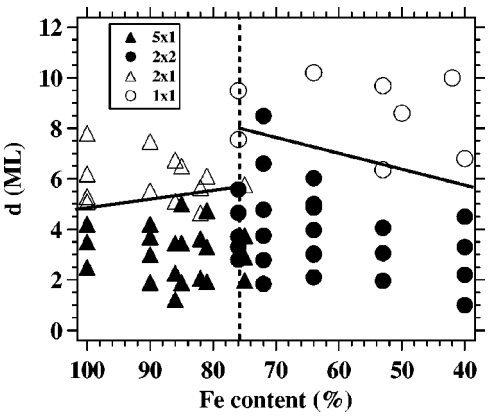

FIG. 5. Symmetry of the LEED pattern of $Fe_xMn_{1-x}/Cu(100)$ alloy films. The lines serve as a guide to separate regions of different properties.

et al. deposited their alloy at 315 K. Second, we employ a growth rate of ~0.2 ML/min compared to 0.5–1 ML/min in their work. These are in our view only modest differences, and it is not clear whether these can explain the different observations. Interestingly when growing a $Fe_{50}Mn_{50}$ alloy onto 8-ML Co/Cu(100) we observed only a $p(1\times1)$ pattern even for a coverage of 1 ML. This result is inline with the reported data of Offi *et al.*[16] Immediately repeating this experiment on Cu(100) did result in the emergence of a $c(2\times2)$ structure below ~6 ML. Since the Co film grows pseudomorphically on Cu(100) the $Fe_{50}Mn_{50}$ alloy experiences the same in-plane lattice constant. Yet the resulting LEED pattern is different. Clearly the chemical/magnetic nature of the substrate plays a role as far as the $c(2\times2)$ pattern is concerned. We would like to add a few comments as to whether the $c(2\times2)$ extraspots have their origin in a contamination of the sample since we generally observe a small C contamination of ~3% in our samples. In a first step we grew a ~6 ML Fe/Cu(100) sample and exposed it then deliberately to a vacuum with an enhanced (by a factor of ~100) CO and CO_2 partial pressure via degassing filaments. Only after an exposure of ~20 L for each species we could observe $c(2\times2)$ spots on the 6 ML Fe/Cu(100) sample. The resulting Auger spectrum showed contamination levels of ~20% and 3% for C and O, respectively. These values are an order of magnitude higher than for our as-grown alloy films. From this result we conclude that the $c(2\times2)$ intensity of the investigated Fe_xMn_{1-x} alloys is not due to contamination. Further evidence comes from the LEED pattern of a 9.7 ML $Fe_{53}Mn_{47}$ sample which does not display spots due to a $c(2\times2)$ structure; see Fig. 3. A contamination induced $c(2\times2)$ structure should also be present at a larger thickness.

Although the misfit is small [see Fig. 1(a)] we expect a tetragonally distorted structure of the alloy films. It is well-established that the LEED *I-V* measurement of the (0,0) spot yield the layer averaged perpendicular lattice constant $d_\perp$,[25] examples are shown in Fig. 6. For a quantitative analysis the following formula is employed to determine $d_\perp$ (Ref. 25):

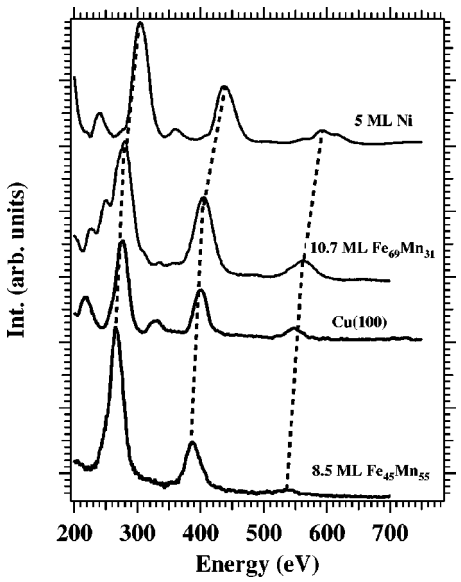

FIG. 6. LEED *I-V* curves of the (0,0) spot for Ni/Cu(100), Cu(100), $Fe_{45}Mn_{55}$, and $Fe_{69}Mn_{31}/Cu(100)$. The dashed lines connect Bragg peaks of the same order.

$$d_\perp = \frac{n\pi\hbar}{\sin\theta\sqrt{2m_e[E(n)-U_0]}}. \quad (1)$$

$E(n)$ is the energy of the Bragg peak with order n and the inner potential is denoted with U_0. The electron mass is labeled with m_e. We estimate the penetration depth to be ~5 ML, this means $d_\perp$ is the average of the first 5 ML. In Fig. 6 we show some selected $I(V)$ curves. Compared to the curve of Cu(100) the $Fe_{69}Mn_{31}$ and $Fe_{45}Mn_{55}$ alloys show a small variation of the bragg peak position. For the latter we see a shift towards smaller energies, which means that $d_\perp$ is larger than for Cu(100). For the $Fe_{69}Mn_{31}$ alloy we observe a shift towards larger energies. Clearly $d_\perp$ has decreased compared to Cu(100). We also show the *I-V* curve for 5 ML Ni/Cu(100) which displays a larger shift. This is a consequence of the larger misfit. The important fact here is that the films are not strictly fcc but tetragonally distorted as expected. We have compiled values of $d_\perp$ for a variety of concentrations. In order to compare bulk and thin films better we have calculated the atomic volume. For the films we assumed pseudomorphic growth; the result is shown in Fig. 7. For the bulk we see that the atomic volume is a linear function of the Fe content. This is matched by the behavior of 10 ML thick alloy films in the concentration interval 45–65 % Fe. We attribute the offset to a systematic error in the determination of $d_\perp$. We notice, however, that there is a clear deviation from a linear curve for higher Fe contents, there the atomic volume is larger than the bulk. Compared to the 10 ML thick films 5-ML-thick specimens have a slightly increased atomic volume. It is of course tempting to ask whether this could be related to a moment-volume instability similar to fcc Fe and Fe_xNi_{1-x} invar alloys.[26,27] In this case it might be possible to drive the Fe_xMn_{1-x} into a ferromagnetic state. Evidence of magnetic order in these samples will be discussed below.

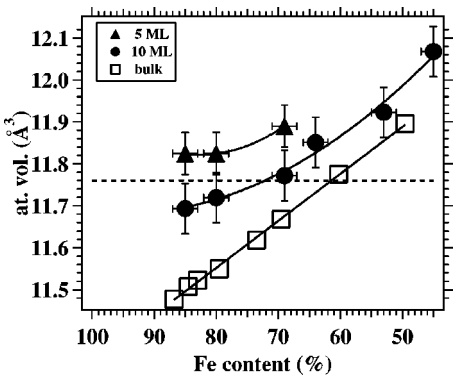

FIG. 7. The concentration dependence of the atomic volume is plotted for 5 ML and 10 ML thick alloy films and the bulk. The dashed line refers to the atomic volume of Cu.[10] The solid lines are guide to the eye.

V. Fe SURFACE SEGREGATION

An important aspect for alloy surfaces and alloy thin films is surface segregation of one constituent.[5–7] In the context of exchange bias it is of course important to determine the concentration at the surface of the antiferromagnetic layer. Consequently we employed Auger spectroscopy to investigate surface segregation for Fe_xMn_{1-x} alloys. In a first step we tested the probing depth of our experiment. For this we investigated a Fe/Cu(100) sample. We collected Auger spectra across the low kinetic energy Auger electrons (47 and 60 eV for Fe and Cu) under various angles of incidence. We then computed the intensity ratio of Cu and Fe Auger peaks. Using the following equation we determined an effective attenuation length λ:

$$\text{ratio} = \frac{I_{Cu}}{I_{Fe}} = \frac{e^{-d/\lambda}}{1-e^{-d/\lambda}}. \tag{2}$$

The numerator describes the attenuation of the Cu Auger intensity due to the Fe layer. The increase of the Fe Auger intensity is given by the denominator. For normal incidence of the electron beam we derive a value $\lambda = 2.2$ ML. If we take into consideration the take-off angle (22°) of the electrons given by the circular aperture our CMA-type spectrometer we get 2.4 ML for the ''true'' attenuation length. This value compares favorable with the value of 2.0 ML determined by Pappas *et al.* for 40 eV photoelectrons on the system Fe/Cu(100).[28] An enhancement of the surface sensitivity is possible if we rotate the sample 55° off-normal. We then derive a value of $\lambda = 0.8$ ML. This means that employing this geometry one will detect contributions within the first two monolayers at most. With this in mind we investigated a $Fe_{54}Mn_{46}$ sample with thicknesses of 2.8 and 7.3 ML. In Fig. 8 we show the Auger spectra for the two different angles of incidence. It becomes immediately clear that the Fe peak has become stronger compared to the Mn peak when rotating the sample from 0° to 55°. This is true for both thicknesses investigated. This means that the segregation is not tied to the appearance of either the $c(2\times2)$ or $p(1\times1)$ pattern. Consequently we have clear evidence of Fe surface segregation. Panel (b) also shows that surface segregation of Cu does not play a role, since at 7.3 ML no Cu peak can be detected. Surface segregation is expected to occur after annealing to 350 K. This temperature is known to be sufficient for Cu surface segregation to occur in such systems as Co/Cu(100) and Fe/Cu(100).[29,30] This is driven by the smaller surface free energy of Cu compared to the film material; this also applies to our case. Because of the fact that we cannot determine the maximum of the Fe Auger peak, the peak-to-peak height cannot be determined. However, we may assume that the maximum of the Fe peak has the same value as for the Mn. Using this approximation for the spectrum obtained at 0° the peak-to-peak ratio of the Fe and Mn peaks is ~ 1, which is equivalent to a 50% Fe content. In the case of the spectrum measured at 55° the peak-to-peak ratio amounts to ~ 1.6 or to 62% Fe. This is a sizeable segregation effect, a more surface sensitive technique could yield an even larger surface concentration since we still sample the second layer. We are not aware of a previous study on the segregation in

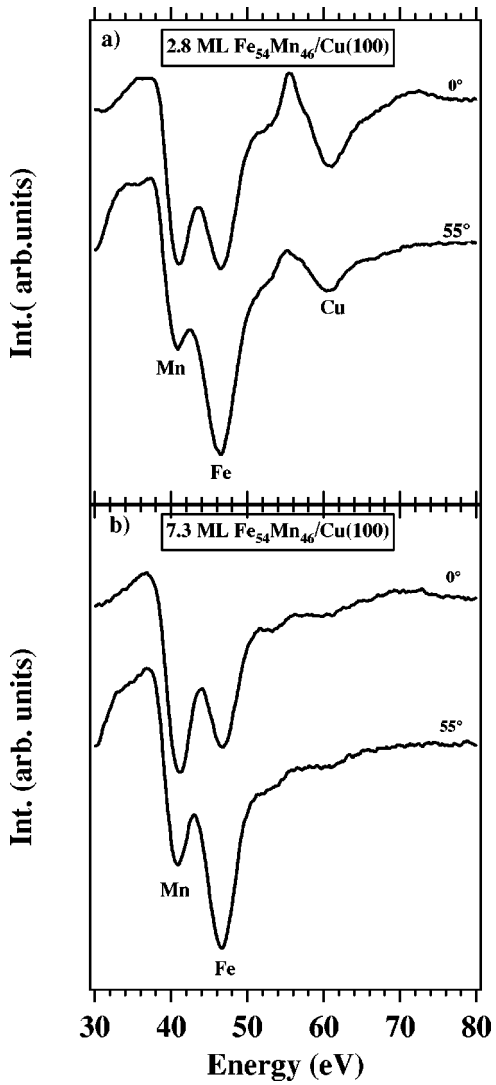

FIG. 8. Auger spectra of a $Fe_{54}Mn_{46}$ alloy. The Auger peaks of Mn, Fe, and Cu are labeled. Panel (a) depicts the spectrum for 2.8 ML, whereas panel (b) shows the spectrum for 7.3 ML.

Fe_xMn_{1-x} alloys despite the extensive use of $Fe_{50}Mn_{50}$ as an antiferromagnetic layer. The use of the bulk spin structure when discussing the exchange bias is already questionable but with the evidence of Fe segregation not warranted. Interestingly publications on the exchange bias in $Co/Fe_{50}Mn_{50}$ systems find evidence of uncompensated Fe moments, which appear to reside at the interface $Co/Fe_{50}Mn_{50}$ and are parallel to the Co moments.[17,31,32] This observation is surprising when considering the bulk spin structure of $Fe_{50}Mn_{50}$. There one expects that the (100) surface has no net moment.[33] It is tempting to determine an estimate of the amount of Fe at the surface. For this we assume that the segregation is located in the first ML. A content of 62% Fe amounts to 0.62 ML of Fe, but only 0.38 ML of Mn reside at the surface. This means that only 0.38 ML Fe are required to form an $Fe_{50}Mn_{50}$ alloy. This yields a remaining value $\sim$0.24 ML ''uncompensated'' Fe, in agreement with XMCD studies.[17,31,32] We conclude that surface segregation can easily explain the ''uncompensated'' Fe. However we have to point out that growth of another metallic layer (e.g., Co) might change the Fe enrichment at the interface. We have tried to investigate this effect by growing up to 3 ML Ni on a $Fe_{50}Mn_{50}$ sample. Thicker Ni films cannot be investigated due to the strong attenuation of Fe and Mn. A Co film would have been more appropriate when comparing with previous XMCD (X-ray Magnetic Circular Dichroism) studies.[17,31,32] However the low kinetic Auger peak of Co is too close to the peaks of Fe and Mn. We find preliminary evidence that the Fe enrichment at the interface $Ni/Fe_{50}Mn_{50}$ is reduced compared the $vacuum/Fe_{50}Mn_{50}$ interface. These facts highlight that a careful chemical analysis of the interface is essential for a discussion of the magnetic properties.

VI. MAGNETIC PROPERTIES OF Fe_XMn_{1-x} FILMS

As discussed in Sec. I bulk fcc Fe_xMn_{1-x} alloys in the concentration interval 50–80 % display antiferromagnetic order. Despite this we are able to detect magnetism via MOKE as we will show now. In Fig. 9 we display polar Kerr loops of an $Fe_{81}Mn_{19}$ alloy. At 1.7 ML we are able to pick up a weak Kerr signal at 110 K though without a remanence, at 290 K reduces the signal level is almost zero. The 2.2 ML sample displays a hysteresis at 110 K the remanence being $\sim$50% of the saturation, which has vanished at 290 K. This means we have exceeded T_C significantly. The 2.7 ML thick sample has a square hysteresis loop at 110 K, at 290 K the remanence is zero though only small fields are required to achieve saturation. This suggests that T_C is close to 290 K. Finally the loops of the 3.5 ML sample are square at both temperatures; consequently T_C must be above 290 K. This first rough estimate of T_C as a function of the thickness d has been confirmed by more careful measurements. In Fig. 10 we show polar loops for a $Fe_{71}Mn_{29}$ and $Fe_{62}Mn_{38}$ sample at 110 K. For the $Fe_{71}Mn_{29}$ sample we detect the first signal at 2.1 ML although the remanence is zero. This curve resembles a hard axis loops, but we cannot pick-up a magnetic signal in-plane. The first loop with low remanence can be observed at 3.1 ML. The remanence increases for thicknesses of 3.6 and 4.1 ML; however, we note that the signal level does not

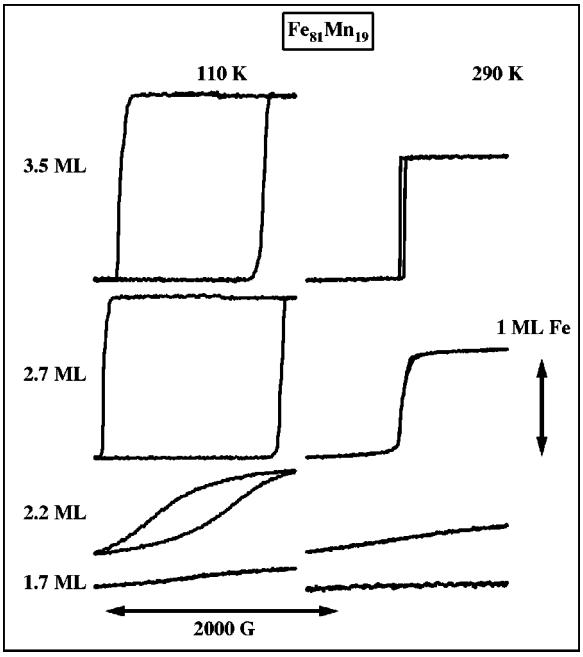

FIG. 9. Selected polar M-H loops from a $Fe_{81}Mn_{19}$ sample at various thicknesses. The loops on the left (right) half are obtained at 110 K (290 K). For comparison of the signal levels we added an arrow indicating the signal equivalent of 1-ML Fe. The height of the loops has been normalized, therefore the signal levels can be directly compared.

increase with thickness, but decreases. Beyond 4.1 ML no signal can be obtained in either field direction. For a $Fe_{62}Mn_{38}$ sample we are also able to detect a magnetic signal when probing the out-of-plane magnetization. However the signal levels are significantly smaller compared to the Fe_{71} sample and no hysteresis is detectable. Even for a $Fe_{50}Mn_{50}$ sample we could detect a magnetic signal in this thickness regime, which was even smaller than the signal levels of the Fe_{62} sample. Further work is in progress to study the properties of alloy samples near an Fe content of 50%.

Having established that the Fe_{81} and Fe_{71} sample display ferromagnetic (or ferrimagnetic) order it would be of interest to determine the Curie temperatures $T_C(d)$. Therefore we performed temperature dependent measurements. From the Kerr loops we determined the temperature dependence of the remanence and identified the vanishing remanence as the Curie point. In the case of perpendicular magnetized samples it should be emphasized that a vanishing remanence is not identical to the Curie point.[34] A multidomain state with domain sizes much smaller than the spatial resolution of the experiment would also yield a zero remanence before T_C is reached. Such a situation has been observed for perpendicular magnetized Ni/Cu(100) films.[34] However the difference in the temperature values where the remanence vanishes and a proper analysis via Arrott plots[35] is only a few percent which we neglect in the following. Our experiments show that T_C of 2.2 ML Fe_{81} is about 180 K the corresponding value for the 2.7 ML sample is $\sim$280 K. Similar experiments have been performed for samples with an Fe content of 72, 67 and 61 %, respectively. The data have been compiled in Table I together with published data on Ni/Cu(100)

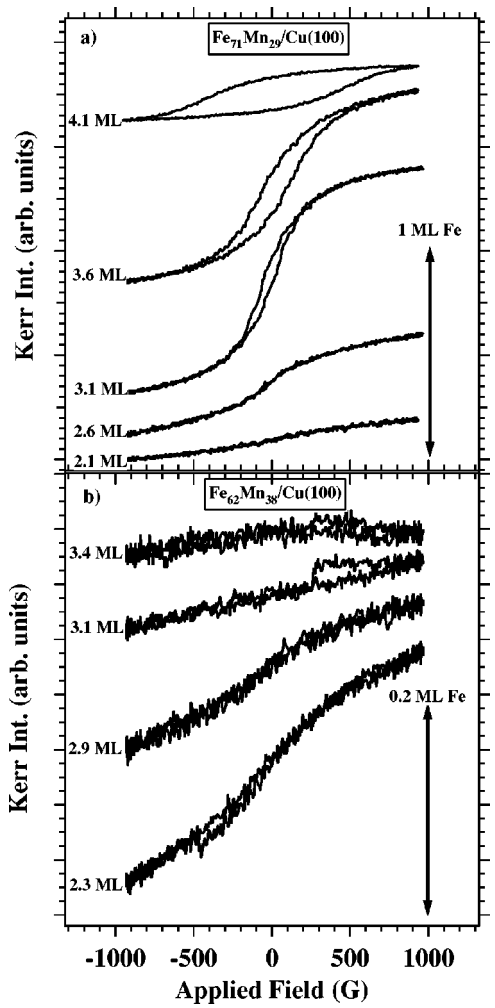

FIG. 10. Selected polar *M-H* loops from a $Fe_{71}Mn_{29}$ and $Fe_{62}Mn_{38}$ sample obtained at 110 K. The signal levels have been normalized therefore the height of the loops can be directly compared for each sample. For comparison of the signal levels we added an arrow indicating the signal equivalent of 1 and 0.2 ML Fe, respectively.

and $Fe_{50}Ni_{50}$.[36,37] We find for all samples (except for the $Fe_{61}Mn_{39}$ alloy) that T_C at a given thickness is above the value of Ni/Cu(100). From this we deduce that the ''bulk'' value of these alloys is above the bulk value of Ni ($\sim$640 K). On the other hand, the data of the $Fe_{50}Ni_{50}$ alloy determine an upper boundary of $\sim$750 K for the infinite thick Fe_xMn_{1-x} alloys. These numbers we can compare now with bulk data; see Fig. 1. We recall that the Néel temperature T_N for fcc Fe_xMn_{1-x} alloys is in the range $\sim$400–500 K, hence below the T_C of Ni. Clearly the ordering temperature of the alloy films is surprisingly high. Additionally we observe ferromagnetic or ferrimagnetic order in contrast to the bulk antiferromagnetic structure.

We have shown above that the atomic volume of 5 ML was larger than 10 ML thick films. It is well known that moment-volume instability exists for fcc Fe and Mn and for fcc Fe_xNi_{1-x} alloys.[26,27,38] For fcc Fe it is well-established that two distinct magnetic phases exist.[26] The one associated with the large atomic volume (large moment) displays ferromagnetic order and is termed HS (high spin). The phase with a small atomic volume (small moment) belongs to an antiferromagneticly ordered state termed LS (low spin). A similar behavior has been predicted for fcc Mn.[26] However, the main difference is that for realistic atomic volumes only antiferromagnetic phases are possible. We expect volume-moment instabilities for fcc Fe_xMn_{1-x} alloys to be present where the HS state becomes eventually an antiferromagnetic state. Although we are not aware of a systematic theoretical study for fcc Fe_xMn_{1-x} alloys confirming this view. Using this argument we may ascribe the observation of magnetic order in ultrathin Fe_xMn_{1-x} films below $\sim$5 ML to a moment-volume instability. At $\sim$10 ML the structure has relaxed and we expect that the bulk properties are adopted namely antiferromagnetic order. On the other hand we have to recall that we have observed Fe surface segregation and a $c(2\times2)$ structure indicative of chemical order. In this context a recent theoretical paper discusses chemically ordered fcc $Fe_{50}Mn_{50}$.[39] They find that the groundstate does have a net magnetization despite strong antiferromagnetic Mn-Mn and Mn-Fe interactions and a weak ferromagnetic Fe-Fe interaction. This provides an alternative explanation for the observation of magnetic signals.

TABLE I. Comparison of thickness dependent T_C values for Fe_xMn_{1-x} alloys and published data on Ni and $Fe_{50}Ni_{50}$ films on Cu(100) (Refs. 36 and 37).

	T_C(K)					
d(ML)	Ni	$Fe_{81}Mn_{19}$	$Fe_{76}Mn_{24}$	$Fe_{72}Mn_{28}$	$Fe_{67}Mn_{33}$	$Fe_{50}Ni_{50}$
2.2	-	180	120	-	-	248
2.4	70	-	-	-	-	-
2.6	-	-	-	-	-	308
2.7	-	280	-	-	-	-
2.8	-	-	210	170	$<$110	-
2.9	110	-	-	-	-	-

VII. SUMMARY

We studied ultrathin Fe_xMn_{1-x} alloy films grown on Cu(100) in the concentration interval 50–80% Fe. There the bulk is stabilized in the fcc phase. Our results are as follows: (i) In agreement with the observations of Offi *et al.* we find good epitaxial growth for Fe_xMn_{1-x}/Cu(100).[16,17] Further, the films are not exactly fcc but in a tetragonally distorted phase. (ii) Our structural studies revealed that for 40–75% Fe content a $c(2\times2)$ symmetry can be observed suggesting an ordered alloy. This transforms into the expected $p(1\times1)$ symmetry in the interval 6–10 ML. Growth on a Co/Cu(100) surface produced alloy samples without a $c(2\times2)$ LEED pattern despite the same in-plane lattice constant as Cu(100). We conclude that the chemical/magnetic properties of the substrate are of relevance for the emergence of the $c(2\times2)$ structure. (iii) We observed that Fe surface segregation plays a role in Fe_xMn_{1-x} alloys. For a $Fe_{54}Mn_{46}$ alloy we estimate an Fe content enhancement of $\sim$10%, resulting in $\sim$0.24 ML of ''uncompensated'' Fe spins. This is in

agreement with studies on ultrathin $Co/Fe_{50}Mn_{50}$ structures investigated with XMCD.[17,31,32] (iv) We detect magnetic order if the thickness is below ~4 ML. Though a remanence can only be observed for Fe contents above 67%. A possible explanation of this could be related to volume-moment instabilities. However, a chemically ordered alloy with a net moment could also be feasible.[39]

Our results show that structure and chemistry of $Fe_xMn_{1-x}/Cu(100)$ films are markedly different from a surface termination of the bulk. These observations are of relevance for further discussions on exchange-bias systems.

ACKNOWLEDGMENT

This work was supported by the DFG, Sfb 290 (TP A11). We thank Dr. J. Lindner for critical proofreading.

[1] J. Nogués and I.K. Schuller, J. Magn. Magn. Mater. **192**, 203 (1999).
[2] H. Ohldag, A. Scholl, F. Nolting, S. Anders, F.U. Hillebrecht, and J. Stöhr, Phys. Rev. Lett. **86**, 2878 (2001).
[3] R. de Masi, D. Reinicke, F. Müller, P. Steiner, and S. Hüfner, Surf. Sci. **515**, 523 (2002).
[4] P. Luches, M. Liberati, and S. Valeri, Surf. Sci. **532-535**, 409 (2003).
[5] K. Wandelt and G. Ertl, J. Phys. F: Met. Phys. **6**, 1607 (1976).
[6] F.O. Schumann, S.Z. Wu, G.J. Mankey, and R.F. Willis, Phys. Rev. B **56**, 2668 (1997).
[7] A. Atrei, U. Bardi, G. Rovida, A. Blashchuk, O. Mishchuk, and M. Vasylyev, Surf. Sci. **478**, 18 (2001).
[8] J.R. Cerda, P.L. de Andres, A. Cebollada, R. Miranda, E. Navas, P. Schuster, C.M. Schneider, and J. Kirschner, J. Phys.: Condens. Matter **5**, 2055 (1993).
[9] W. Platow, U. Bovensiepen, P. Poulopoulos, M. Farle, K. Baberschke, L. Hammer, S. Walter, S. Müller, and K. Heinz, Phys. Rev. B **59**, 12 641 (1999).
[10] W.B. Pearson, *Handbook of Lattice Spacings and Structures of Metals* (Pergamon Press, Oxford, 1958).
[11] H. Yamauchi, H. Watanabe, Y. Suzuki, and H. Saito, J. Phys. Soc. Jpn. **36**, 971 (1974).
[12] U. Gonser, C.J. Meechan, A.H. Muir, and H. Wiedersich, J. Appl. Phys. **34**, 2373 (1963).
[13] H. Zähres, M. Acet, W. Stamm, and E.F. Wassermann, J. Magn. Magn. Mater. **72**, 80 (1988).
[14] J. Thomassen, F. May, B. Feldmann, M. Wuttig, and H. Ibach, Phys. Rev. Lett. **69**, 3831 (1992).
[15] D. Qian, X.F. Jin, J. Barthel, M. Klaua, and J. Kirschner, Phys. Rev. Lett. **87**, 227204 (2001).
[16] F. Offi, W. Kuch, and J. Kirschner, Phys. Rev. B **66**, 064419 (2002).
[17] F. Offi, W. Kuch, L.I. Chelaru, K. Fukumoto, M. Kotsugi, and J. Kirschner, Phys. Rev. B **67**, 094419 (2003).
[18] D. Tian, S.C. Wu, and F. Jona, Solid State Commun. **70**, 199 (1989).
[19] D. Tian, R.F. Lin, F. Jona, and P.M. Marcus, Solid State Commun. **74**, 1017 (1990).
[20] M. Wuttig, Y. Gauthier, and S. Blügel, Phys. Rev. Lett. **70**, 3619 (1993).
[21] T. Flores, M. Hansen, and M. Wuttig, Surf. Sci. **279**, 251 (1992).
[22] W.L. O'Brien and B.P. Tonner, Phys. Rev. B **51**, 617 (1995).
[23] S. Müller, P. Bayer, C. Reischl, K. Heinz, B. Feldmann, H. Zillgen, and M. Wuttig, Phys. Rev. Lett. **74**, 765 (1995).
[24] R. Thamankar, S. Bhagwat, and F.O. Schumann, Phys. Rev. B (to be published).
[25] J.B. Pendry, *Low Electron Energy Diffraction* (Academic Press, New York, 1974).
[26] V.L. Moruzzi, P.M. Marcus, and J. Kübler, Phys. Rev. B **39**, 6957 (1989).
[27] I.A. Abrikosov, O. Erikson, P. Söderlind, H.L. Skriver, and B. Johansson, Phys. Rev. B **51**, 1058 (1995).
[28] D.P. Pappas, K.P. Kämper, B.P. Miller, H. Hopster, D.E. Fowler, C.R. Brundle, A.C. Luntz, and Z.X. Shen, Phys. Rev. Lett. **66**, 504 (1991).
[29] M.T. Kief and W.F. Egelhoff, Jr., Phys. Rev. B **47**, 10 785 (1993).
[30] J. Thomassen, B. Feldmann, and M. Wuttig, Surf. Sci. **264**, 406 (1992).
[31] W.J. Antel, F. Perjeru, and G.R. Harp, Phys. Rev. Lett. **83**, 1439 (1999).
[32] F. Matthes, A.A. Rzhevskii, L.-N. Tong, L. Malkinski, Z. Celinski, and C.M. Schneider, J. Appl. Phys. **93**, 6504 (2003).
[33] R. Jungblut, R. Coehoorn, M.T. Johnson, J. aan de Stegge, and A. Reinders, J. Appl. Phys. **75**, 6659 (1994).
[34] P. Poulopoulos, M. Farle, U. Bovensiepen, and K. Baberschke, Phys. Rev. B **55**, R11 961 (1997).
[35] A. Arrott, Phys. Rev. **108**, 1394 (1957).
[36] K. Baberschke, Appl. Phys. A: Mater. Sci. Process. **62**, 417 (1996).
[37] F.O. Schumann, S.Z. Wu, G.J. Mankey, and R.F. Willis, J. Appl. Phys. **79**, 5635 (1996).
[38] M. van Schilfgaarde, I.A. Abrikosov, and B. Johansson, Nature (London) **400**, 46 (1999).
[39] D. Spišák and J. Hafner, Phys. Rev. B **61**, 11 569 (2000).